THE PHOTOGRAMMETRIC RECORD

The Photogrammetric Record 29(148): 434–453 (December 2014)
DOI: 10.1111/phor.12082

MOTION BLUR DISTURBS – THE INFLUENCE OF MOTION-BLURRED IMAGES IN PHOTOGRAMMETRY

T. Sieberth (T.Sieberth@lboro.ac.uk)
R. Wackrow (R.Wackrow@lboro.ac.uk)
J. H. Chandler (J.H.Chandler@lboro.ac.uk)
Loughborough University, Loughborough, UK

Abstract

Unmanned aerial vehicles (UAVs) have become an interesting and active research topic for photogrammetry. Current research is based on images acquired by UAVs which have a high ground resolution and good spectral resolution due to low flight altitudes combined with a high-resolution camera. One of the main problems preventing full automation of data processing of UAV imagery is the unknown degradation effect of blur caused by camera movement during image acquisition. The purpose of this paper is to analyse the influence of blur on photogrammetric image processing. Images with precisely known motion blur were produced to determine the effect. It was found that even small blurs affect normal photogrammetric processes significantly. Although operator intervention might be time consuming, it can ensure that the results are still of acceptable accuracy.

Keywords: automation, blur, bundle adjustment, camera calibration, image processing, photogrammetry, UAV

Introduction

A constraint enforced on the acquisition of early photographs used in photogrammetry was a stable camera position and a stationary object as the basic requirements for sharp images. Exposure times of many days were required to obtain an image (Maison Nicéphore Niépce, 2013). Today, professional photographers use a tripod and remote shutter release to prevent camera movement during image acquisition.

Unfortunately, unmanned aerial vehicles (UAVs) rarely provide a stable camera position. UAVs are affected by wind, turbulence, sudden input by the operator and also by the flight movement of the aircraft itself. However, their good manoeuvrability and flight path control, combined with endurance, flight range and low cost, make UAVs an appropriate platform for a range of different applications (Eisenbeiss, 2009). Nevertheless, limited payload, regulatory restrictions and vulnerability of the UAV platform encourage the use of low-cost sensors, which dictates the use of consumer-grade cameras (Eisenbeiss, 2011; Eisenbeiss and Sauerbier, 2011). Unfortunately, the problem remains that the high spatial resolution of an image is often degraded due to motion blur. Fig. 1 represents an image acquired using a fixed-wing UAV at an altitude of approximately 100 m above

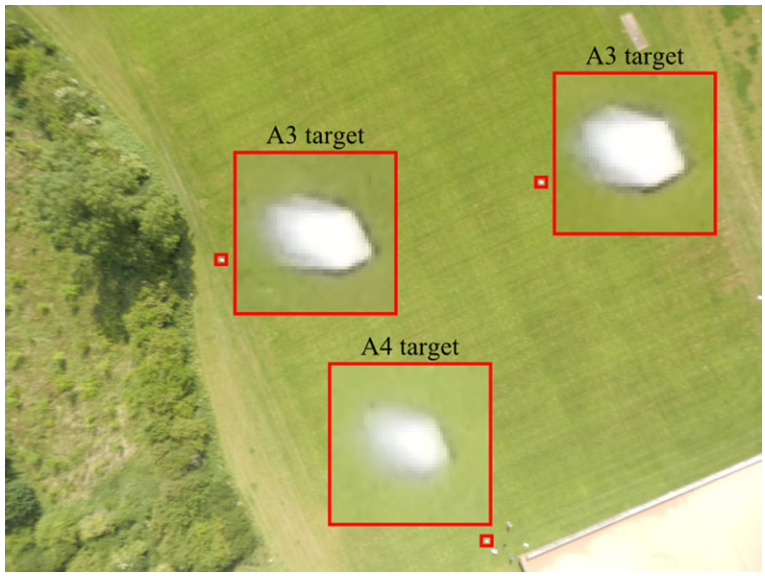

FIG. 1. A 16-megapixel image acquired by a UAV. The three insets show 20-times enlargement of the targets. Targets are blurred due to the forward motion of the UAV.

ground. A Nikon Coolpix S800c was used with the film speed set to ISO 125, which was chosen to achieve the best image quality with the least noise. The magnified insets in Fig. 1 represent blurred targets caused by forward motion of the UAV. However, rotational movements appear to have an even larger influence on the image sharpness than translational movements (Grenzdörffer et al., 2012).

Image sharpness degraded by motion blur is, amongst other effects, visible by a reduction in contrast, which can also be caused by noise or other processes influencing the radiometry of an image. Many of these influences are part of the hardware processing after the image is "on the camera sensor" and would influence a sharp image in the same way as a blurred image. Expressing the sharpness of a motion-blurred image, using a modulation transfer function (MTF) or similar sharpness curves, is problematic as they would return different results depending on the direction of measurement. To overcome this problem, motion blur is expressed in a scale-invariant manner as the physical movement of the camera body in millimetres.

This paper describes the effect of image blur on automatic image processing. Motion-blurred images have been generated to investigate their effect on automatic camera calibration and the functionality of coordinate calculations. The purpose is to define a threshold representing the maximum amount of image blur which is acceptable for automatic processing.

RELATED WORK

Photogrammetry is the science of reconstructing "the position, orientation, shape and size of objects from pictures" (Kraus, 2007, page 1). Aerial photogrammetry uses object

information in images acquired by airborne platforms ranging from aircraft to balloons. A major difference to close range photogrammetry is the normally unstable camera position due to a moving platform. The recently developed UAVs, which are increasingly popular for image flights, are especially vulnerable to wind and turbulence, and are sensitive to user navigational input.

For a successful image flight it is necessary to carefully prepare a flight plan beforehand. To provide appropriate image geometry for 3D measurements a recommended image fore-and-aft overlap (forward – along track) of 60% and a lateral overlap (sidelap – across track) of 20% should be used (Kraus, 2004; Luhmann et al., 2014). To calculate accurate 3D coordinates (X, Y, Z) for an object point, it is necessary to precisely measure the image coordinates (x, y) in at least two images. Today, fully automated data processing is demanded by an increasing number of users.

A series of methods have been developed in previous work to detect if an image is sharp or blurred. It is recognised that improving the image sharpness using deblurring algorithms is an important topic in computer vision and image processing. A widely used application for automatic blur detection is the "autofocus" system in cameras, which should prevent the user from taking optically blurred images caused by an inappropriate focal length setting (Kim and Paik, 1998). As optical blur can be prevented using these systems, other methods are required to suppress blur due to motion, which should be carefully distinguished as a discrete type of blur. Motion blur is often caused by human hand movement (jitter). This jitter has frequencies of 2 to 10 Hz with amplitudes of up to 1 mm (Stiles, 1976). Sachs et al. (2006) note that there is also a "drift of the hand" of up to 5 mm/s and that commercial systems for shake reduction use gyroscopes to prevent motion blur. Methods developed for aircraft use precise inertial measurement unit (IMU) and global navigation satellite system (GNSS) information to reduce angular and forward-motion blur (Pacey and Fricker, 2005). Such systems are expensive and cannot always be used since these would exceed the payload of typical UAV platforms. Furthermore, the IMU and GNSS sensors incorporated for flight stabilisation are not accurate enough and lack sufficient acquisition frequency to determine if an image is blurred or not. However, both sensors can provide additional information for blur detection algorithms such as the approximate path followed when the image was blurred.

Algorithms used for blur detection often use edge detection or frequency analysis. Edge detection methods focus on the spread and gradient of an edge (Ong et al., 2003; Joshi et al., 2008; Narvekar and Karam, 2009). In the case of a widely spread edge of low gradient it is first assumed that the image is blurred. This edge smear due to blur is also used in image frequency analysis methods. When an image has extensively smeared edges in the spatial domain it is characterised by the disappearance of high frequencies in the frequency domain (Liu et al., 2008; Rahtu et al., 2012). A problem with most blur detection methods is the presumption that the image is blurred. Another more important problem is that these blur detection methods are developed using mathematically blurred images without any relation to geometrical motion blur or random hand-held camera shake. In such circumstances the amount of blur is unknown and has to be evaluated subjectively. In an example presented by Shaked and Tastl (2005) (Fig. 2), image (a) is declared sharper than image (b). However, image (b) is at a different scale and contains more detail than (a), as it is possible to identify individual hair strains or differentiate between the shirt collar and the shirt itself. It is obvious that although subjective evaluation of blur is useful, it can be wrong. This explains the desire to develop a

(a) (b)

FIG. 2. A portrait taken with different cameras in a similar scene by Shaked and Tastl (2005).

measure of blur, by generating images with a precisely known image blur which is not influenced by human perception.

METHOD DEVELOPMENT

To quantify the impact of image blur on automatic image processing, images with a precisely known blur are required. In the study described in this paper, three datasets were produced using a shaker table (Fig. 3), which is a device normally used by construction engineers to test the strength of building materials and their resistance against earthquakes or other vibrating influences. In this study, a Nikon D80 camera was mounted on the shaker table and shaken with a known amplitude and frequency. Exposures were synchronised to this movement and images with precisely known blur could therefore be captured (Sieberth et al., 2013).

The first dataset consisted of convergent images of a calibration field comprising 54 coded targets and a Siemens Star in the image centre (Fig. 4(a)). The Siemens Star provides a directly visual way to evaluate both the amount and direction of blur. Coded targets were used to allow for fully automatic camera calibration.

The second dataset consisted of images of a 3D model which include 130 signalised targets and 6 coded targets. The coded targets were located around the 3D model to establish a stable local coordinate system and to evaluate the accuracy of automatically calculated 3D coordinates of the target points (Fig. 4(b)).

The third dataset consisted of differently sized signalised targets obtained with different camera-to-target distances and acquired using both a Nikon D80 and a Nikon D7000

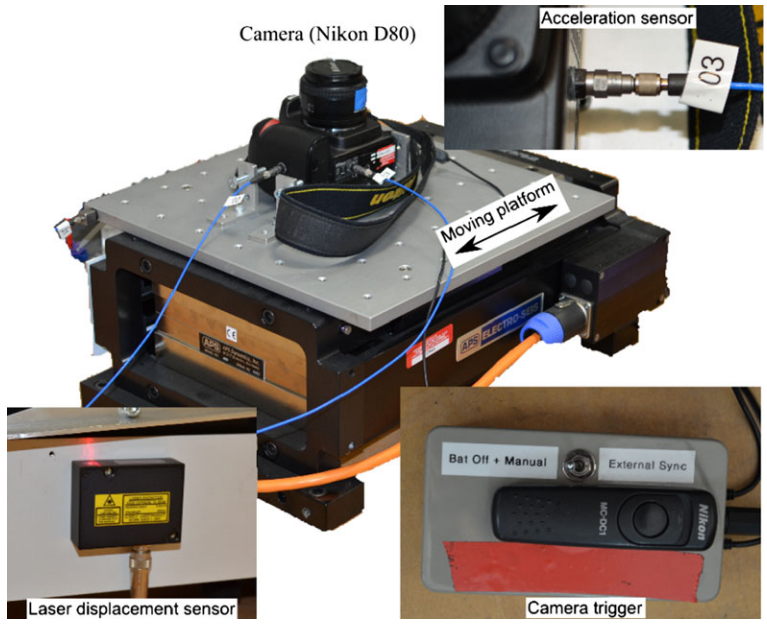

FIG. 3. Representation of the experimental set-up of the shaker table (Sieberth et al., 2013).

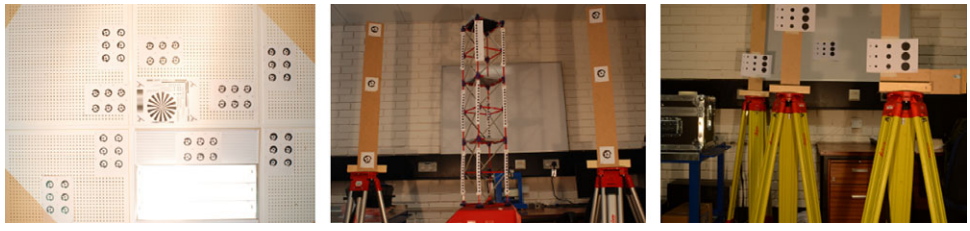

(a) (b) (c)

FIG. 4. Images used in the three datasets: (a) sharp image from the first dataset with the camera pointing towards a ceiling; (b) sharp image from the second dataset with the camera facing horizontally towards a wall; (c) sharp image from the third dataset with the camera also pointing horizontally towards a wall.

camera (Fig. 4(c)). This dataset was used to assess the accuracy of detection of target points.

Terminology

For analysing these datasets it is important to distinguish between the meaning of the terms "measurement", "detection", "identification" and "referencing". "Detection" is the process of finding a target in an image. As targets used in photogrammetry are often of a circular shape, a detection algorithm looks for round objects in the image. It finds the boundaries of a circle and then uses techniques to calculate the centre of the circle (Luhmann, 2014). The detection process can be carried out in two ways: fully automatic,

where the algorithm processes the complete image trying to find targets; or semi-automatic, where the operator defines a region of interest and adjusts search parameters. The latter case was the approach mostly adopted to detect targets in this study. The process of detection is important as the results of the recognised target are subsequently used to calculate the centre of the detected area and derive a "measurement" which is hopefully of sub-pixel precision and represents the actual measured location of the target in the plane of the image. However, if the target is not detected, or incorrectly detected, then no automatic measurement is possible or the measured coordinates will be incorrect. If automatic "measurements" are unsuccessful it is still possible to manually measure coordinates in the image. However, manual measurements are rarely practicable and it is more important to successfully detect a target to ensure automation and sub-pixel measurements.

With an automatically detected and measured target it might be also possible to carry out identification. The term "identification" will be used in this paper to refer to the process of assigning an identifying integer (ID) to a target. This is normally achieved automatically using a coded bit pattern surrounding the target and the code needs to be clearly readable to prevent incorrect identification (Shortis and Seager, 2014). An identified target can then be referenced. "Referencing" is the process of connecting identical targets across multiple images. This can be achieved by using the ID of identified targets.

Influence of Blur on Camera Calibration

The first dataset was used for automatic camera calibration calculation (Table I). To generate a complete image set for camera calibration, images from four stable positions around the shaker table were acquired, each with four different orientations (Fig. 5). These 16 calibration images were acquired with the camera mounted on a tripod and triggered remotely to avoid the introduction of any blur from this source. Around 2000 images with varying blur were taken using the shaker table. Of these 2000 images, 13 images with a camera displacement ranging from no movement up to 1·03 mm were chosen for further analysis.

The process of camera calibration was conducted using the software "PhotoModeler Scanner" (Version 2013·0·3·1131 (64 bit) dated 17th July 2013), which required a minimum of six images for processing. These six images were composed of a subset of five images from the stable camera positions and a sixth image from the shaker table position. A total of 13 image sets with each of the chosen blurred images were processed. Either fully automatic camera calibration was possible or manual intervention was required, depending on the amount of image blur introduced by the shaker table. Intervention involved operator input to semi-automatically detect and measure the blurred targets, which the algorithm was unable to detect, identify and measure.

TABLE I. A list of parameters for the camera calibration dataset.

	Dataset 1
Camera-to-object distance	1·80 m
Size of targets	8 mm
Number of coded targets	54
Focal length	25·35 mm
Aperture	f/8
Frames per process	6
Number of camera displacements analysed	13

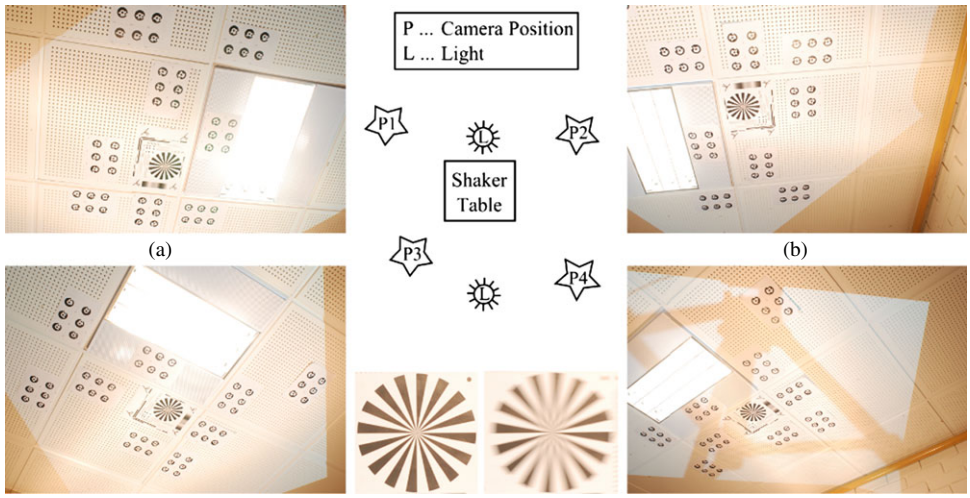

FIG. 5. Sketch of the shaker table set-up: (a) to (d) images from the four stable camera positions P1 to P4; (e) Siemens Star in a sharp image; (f) Siemens Star of the most blurred image with 1·03 mm camera displacement (168·6 sensor pixels).

Automated camera calibration becomes increasingly problematic as PhotoModeler is unable to automatically detect targets in the blurred image. Initial problems for fully automatic target detection occurred with a camera displacement larger than 0·263 mm (Fig. 6(a)), where the algorithm detected only 46 out of 54 targets. With a displacement of more than 0·377 mm (Fig. 6(b)) the number of detected targets was reduced to a point where calibration was no longer possible (Fig. 6(c)).

Additionally, referencing targets identified in the blurred images to targets detected in the sharp images was incorrect due to wrongly identified target numbers. Fig. 7(a) shows

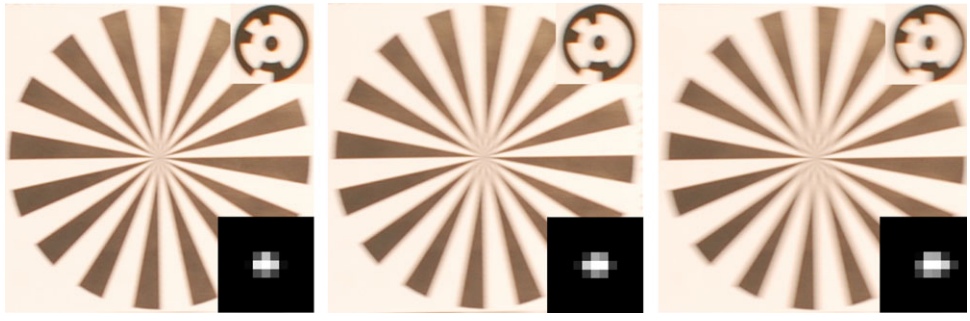

FIG. 6. Siemens Stars and coded targets affected by different motion: (a) camera displaced by 0·263 mm; (b) camera displaced by 0·377 mm (the last fully automatically processed image); (c) with the camera displaced 0·529 mm it is not possible to carry out fully automatic camera calibration. The insets (bottom right in each case) show the blur kernel calculated for these images.

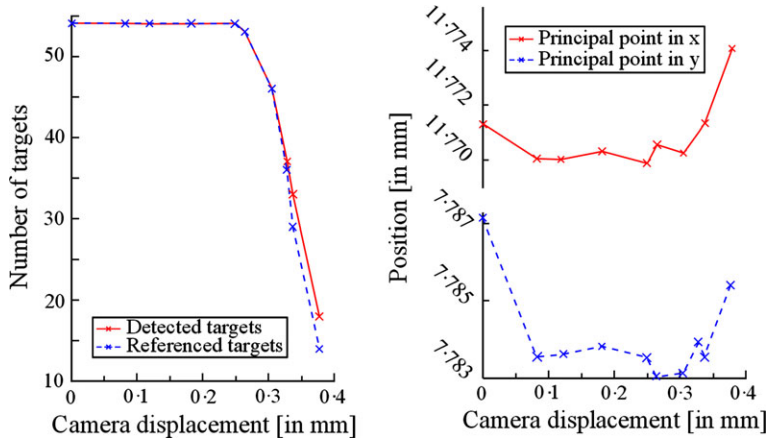

FIG. 7. (a) Number of detected and referenced targets and its dependency upon camera displacement. (b) Influence of camera displacement upon the calculated principal point position.

the number of detected targets and how many of them were referenced. Fig. 7(b) shows the estimated position of the principal point; it appears that it changes its position with increasing blur, although this may be due to the decreasing number of detected targets. To ensure that the camera calibration results were not just influenced by the decreased number of detected targets, semi-automatic detection and measurement of targets was performed using the "sub-pixel target mode" provided by PhotoModeler (Fig. 8). Unfortunately, identification fails completely because it is no longer possible to read the code. However, the "sub-pixel target mode" tool can be applied precisely on the centre dot of a coded target (Fig. 8(d)) for accurate detection and measurement (Figs. 8(e) and (f)).

If the search box of the targeting mode was not applied precisely (Fig. 8(a)), target detection and subsequent target measurement were unsuccessful (Figs. 8(b) and (c)). Manual creation of the detection box at the correct position with the right size is therefore prone to error and is also time consuming. Thus, referencing these targets needs to be carried out manually too. After this manual intervention, all targets have been detected and it was possible to assess the impact of blur created by camera displacement alone. With all targets correctly detected, calibrations can be conducted under conditions similar to a camera calibration using sharp images. Corrections calculated during the process can be distributed to all targets and variations in results can be attributed to blur.

Influence of Blur on Coordinate Calculation

A second dataset (Table II) was generated to assess the influence of blurred targets on coordinate calculations. A Nikon D80 camera was calibrated and used to acquire data for this specific study. A sharp image from a stable camera position beside the shaker table was acquired. Afterwards the camera was fixed on the shaker table and 328 images with varying blur were acquired. A subset of six images, with camera displacements from no movement up to 1·51 mm were used. The 3D coordinates of control points, the sharp image from the position next to the table and one of the six chosen blurred images from the shaker table position were included to evaluate the influence of blur on coordinate calculations.

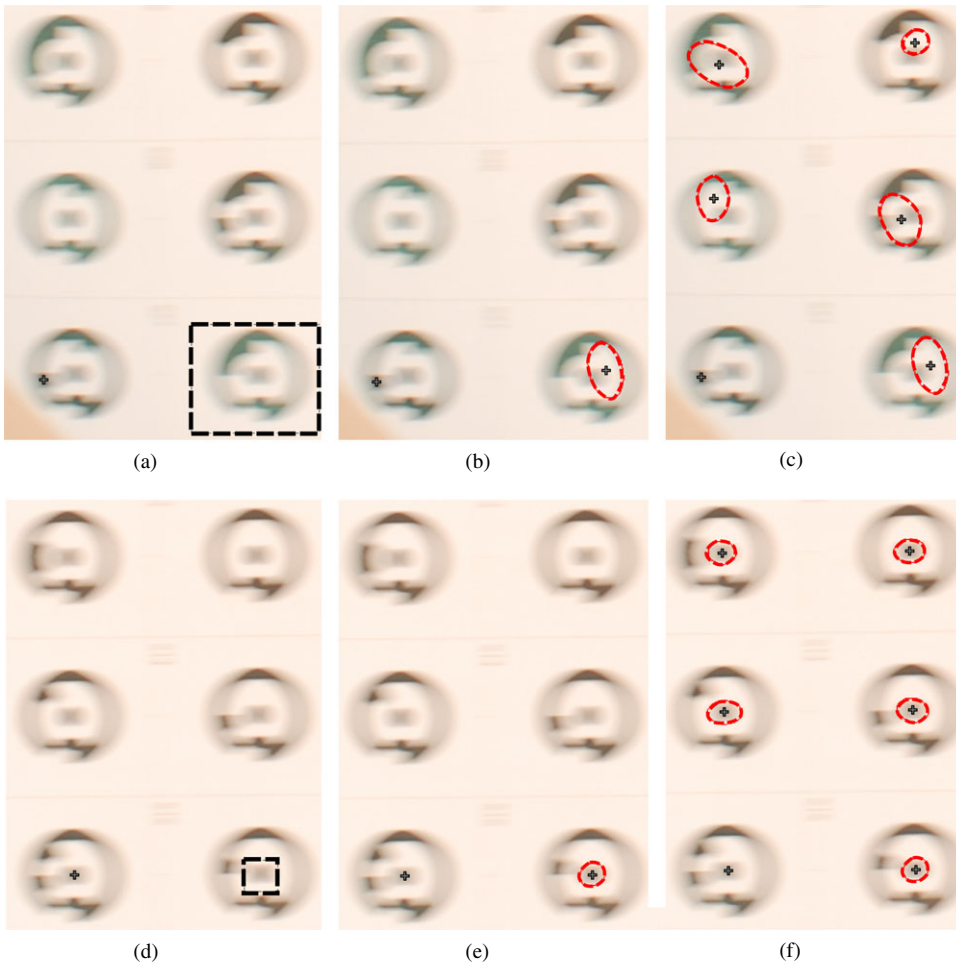

FIG. 8. Example of target detection on the most blurred image: (a) and (d) sub-pixel targeting area which was used; (b) and (e) the result of the detection and measurement; (c) and (f) the result of similar tests with search areas equivalent to those shown in (a) and (d). More successful detection and measurement can be achieved by using smaller target areas (d).

At first, the coded control points had to be detected, identified and measured. In addition to the detection and identification of the coded targets, it is now necessary to detect the uncoded targets on the model (Fig. 4(b)). Similarly to the results found with the first dataset, automatic detection of targets becomes unreliable with increasing blur. Eventually, detection and referencing between sharp and blurred images becomes impossible. When problems occurred using the "automatic target marking" tool, semi-automatic detection of each point was performed using PhotoModeler's "sub-pixel target mode" tool. Although appearing successful, Fig. 9(a) shows that the detection of circles can be inaccurate due to the blur. However, automatic measurement generally derives a point close to the centre of the blurred target. Difficulties encountered in automatic target detection and measurement shown in Fig. 9(b) seem to be caused by the appearance of two target silhouettes caused by

TABLE II. A list of parameters for the coordinate calculation dataset.

	Dataset 2
Camera-to-object distance	1·70 m
Size of targets	9 mm
Number of coded targets	6
Number of uncoded targets	130
Focal length	28·86 mm
Aperture	f/14
Frames per process	1 blurred + 1 sharp image
Number of camera displacements analysed	6 (+1 blur repeatedly used for manual target measurements)

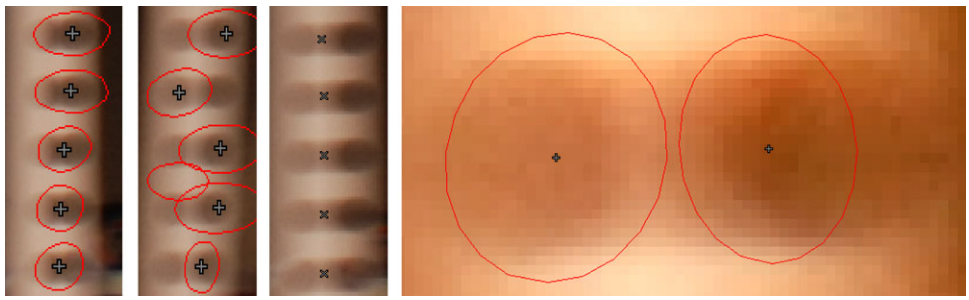

FIG. 9. Example of PhotoModeler's "sub-pixel target mode" tool on the most blurred images of the second dataset: (a) detection with 0·99 mm camera movement appears to be successful; (b) detection with 1·51 mm camera movement is strongly affected by blur; (c) manual measurement appears to be more accurate but is also more time consuming; (d) appearance of two dots per target compromises the accuracy of the automatic detection.

a large degree of blurring. An alternative explanation is the combination of a black target on a dark background. Fig. 9(d) represents an example where the right silhouette appears to be darker than the left because of the darker background at the right-hand side of the target. Due to the motion, the black background is mixed with the target and appears as a second, darker, target. This appearance of two targets can be solved by manual measurement (Fig. 9(c)) or by using methods which detect both circles and calculate the middle between both (Boracchi et al., 2007).

A critical aspect is target referencing between images. Referencing targets between images automatically becomes increasingly difficult with larger blurs (Table III). This is caused by the problem of finding similar features in both images to generate a unique identification because blurring makes identification of suitable features more difficult. Features are normally defined by edges but due to blurring they are not similar in both images. Finally, 3D coordinates can be determined and the effect of various degrees of blur can be established in the object space.

Influence of Blur on Target Detection

The third dataset was acquired to analyse the influence of blur on automatic target detection (Table IV). Targets of different sizes were placed at different distances, and

TABLE III. Influence of camera movement on automatic detection and referencing of uncoded signalled targets.

Camera movement (mm)	*Number of "automatic target marking" targets out of 128*	*Automatic referenced targets out of 126*
0	132 (4 wrong)	125
0·2012	130 (2 wrong)	96 (4 wrong)
0·3176	135 (8 wrong)	84 (3 wrong)
0·4923	126 (3 wrong)	69 (4 wrong)
0·9900	0	80 (1 wrong)
1·5134	0	11 (7 wrong)
1·5134 (manual measured targets)	0	41 (3 wrong)

TABLE IV. A list of parameters for the dataset to analyse the influence of blur on target detection.

	Dataset 3
Camera-to-object distances	1·70 m; 2·10 m; 2·70 m; 3·20 m
Size of targets	4 mm; 10 mm; 19 mm; 35 mm
Number of uncoded targets	48
Focal lengths	25·97 mm (Nikon D80); 29·31 mm (Nikon D7000)
Aperture	f/14
Number of camera displacements analysed	14 (Nikon D80); 15 (Nikon D7000)

images with different camera models and lenses were acquired. Two cameras were mounted on the shaker table: a Nikon D80 with a 24 mm lens and a Nikon D7000 with a 28 mm lens. The higher camera resolution and focal length of the D7000 provided images with a higher geometric resolution than the D80 images. Targets with diameters between 4 and 35 mm were placed at distances between 1·70 and 3·20 m from the camera (Fig. 10).

At first, the pixel width of each target at each distance was manually counted in the sharp image (Fig. 10(a)). Then automatic detection of signalised points was applied which proved to be successful for all targets except for the smallest targets at the greatest distance (4 mm targets at 3·20 m). At this distance the targets appear to be too small to be detected.

Then automated target detection was applied on the blurred images (Fig. 10(b)), to evaluate whether each target was detected. If detection failed for all three targets of the same size at the same distance, the target pixel width due to motion blur was manually counted. The discrepancy between blurred and sharp target widths was related to the displacement necessary to cause automatic detection to fail.

EVALUATION OF EXPERIMENTAL RESULTS

The prime purpose of the experimental work and subsequent evaluation was to investigate whether blur disturbs normal photogrammetric procedures or not.

Camera Calibration Dataset

The camera calibration dataset (dataset 1) demonstrates that blur certainly has an influence on the level of automation achievable during camera calibration in two ways. First, misidentification of targets occurs, which can result in incorrect referencing of targets between the images. Second, misdetections and subsequently mismeasurement influences the coordinate calculation. Processing 54 photogrammetric targets which are blurred resulted in a

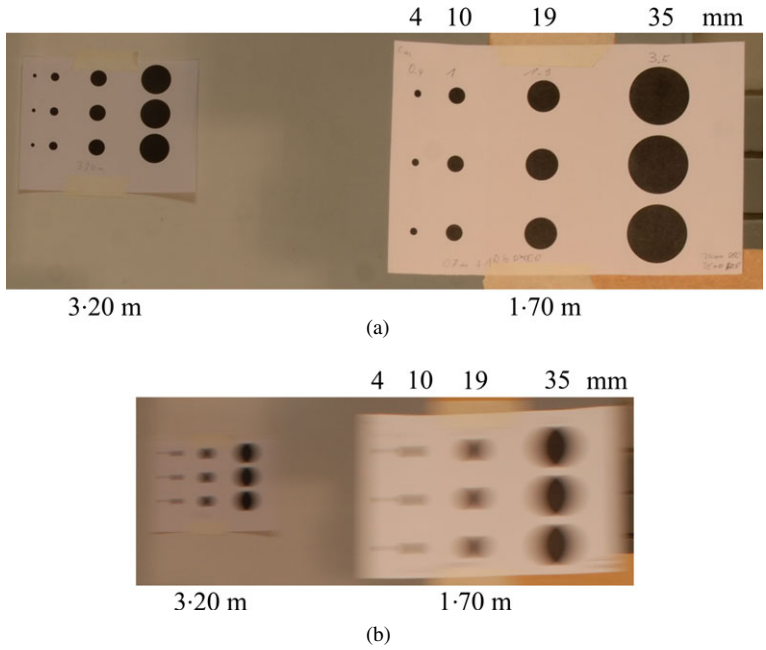

FIG. 10. Example of blurred targets (4 to 35 mm diameter) at different distances: (a) images acquired with a Nikon D7000 camera showing, on the right, a short distance (1·70 m) image and, on the left, far distance (3·20 m) targets in a sharp image; (b) images acquired by a Nikon D80 camera showing equivalent targets in a blurred image. The different sizes of the images are a result of different ground sampling distances.

small change in the camera calibration parameters compared with sharp images (Fig. 7(b)). The decreased accuracy of automatic target measurement can be illustrated by the change of the principal point position (Fig. 11(a)) and the variation in calculated image size (Fig. 11(b)). The figure shows that the calculated image width has a tendency to increase with larger blur. This can be explained perhaps by the shake direction, which is along the x axis.

A detection algorithm attempts to detect the edges of a target. It will find edges that are aligned in the direction of blur easily, because these edges are less affected by blur. In contrast, edges perpendicular to the blur direction create a transitional effect between the target and background, making the detection of edges difficult. Subsequent estimation of the middle, between the start and end of the target, becomes inaccurate and the measured centre does not represent the true target centre. Due to this incorrect detection, subsequent measurements are imprecise, especially in the direction of blur. Measurements derived perpendicularly to the blur direction remain uninfluenced. As these images are blurred along the x axis, x coordinates are the most likely to be inaccurate. It is, perhaps, surprising that the principal point does not change its position on the x axis but varies by about 8 μm on the y axis. There is no obvious explanation for this observation.

These variations in principal point position and estimated image size are insignificant and were not considered as a problem. However, these imply a deteriorating tendency with blur as may be expected. The failure of fully automatic detection and the requirement of semi-automatic target detection also implies that greater blur will cause increasing problems for automated photogrammetric processing.

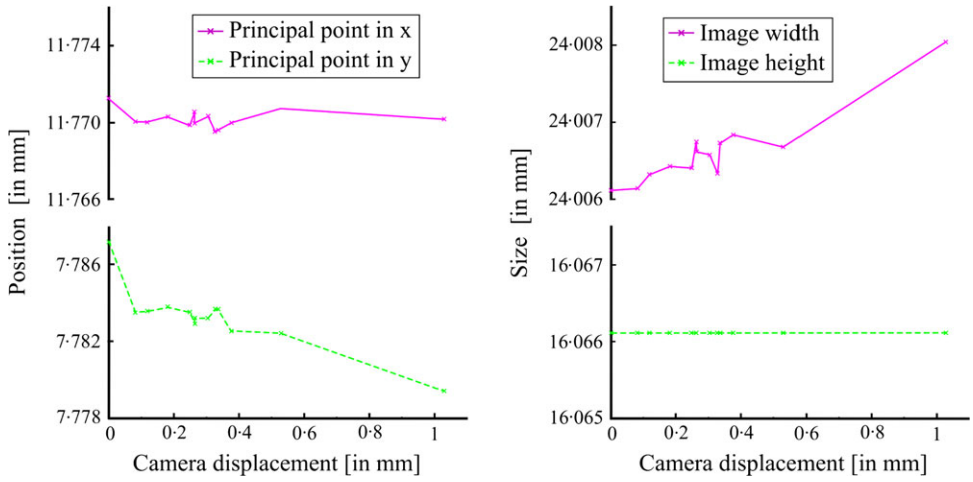

FIG. 11. Influence of image blur on camera calibration results. (a) The movement of the principal point. Contrast this with Fig. 7(b), where the principal point makes a "jump" at a camera displacement of 0·39 mm. (b) Change of the image size with camera displacement.

Coordinate Calculation Dataset

The second dataset used to calculate 3D coordinates also supports the findings of the camera calibration dataset. A small degree of blur prevents fully automatic detection and requires manually assisted or semi-automatic detection. A baseline of 0·82 m and distance of 1·70 m should provide an appropriate intersection angle for precise coordinate calculation. However, the calculated coordinates are inevitably influenced by increased motion blur. As expected, increasing blur creates larger discrepancies between the sharp and blurred coordinates (Fig. 12). Images with a small but apparently invisible blur of up to 0·5 mm are influenced less and create discrepancies in the object space of up to 0·4 mm (Fig. 12(a)). The actual camera displacement of 0·5 mm, divided by the pixel size on the sensor, equals 82 sensor pixels of blur. A 1·5 mm camera displacement is clearly visible to the human eye. This blur results in coordinate discrepancies of up to 20 mm between sharp and blurred images (Fig. 12(b)). In comparison, a fully manual target measurement results in a discrepancy of only 2 mm. This shows that, in the case of visible blur, automatic measurement is clearly inferior to manual measurement.

It can be assumed that larger camera-to-object distances, with both the same baseline and camera displacement, will cause larger errors due to an increasingly smaller intersection angle. A test using the higher resolution Nikon D7000 camera shows the same result of increasing discrepancies for increasingly blurred images.

Target Detection Dataset

While working with the first two datasets, it was observed that target detection in blurred images can be time consuming if semi-automatic detection and measurement is required. Tests reveal that relatively small camera displacements cause automatic target

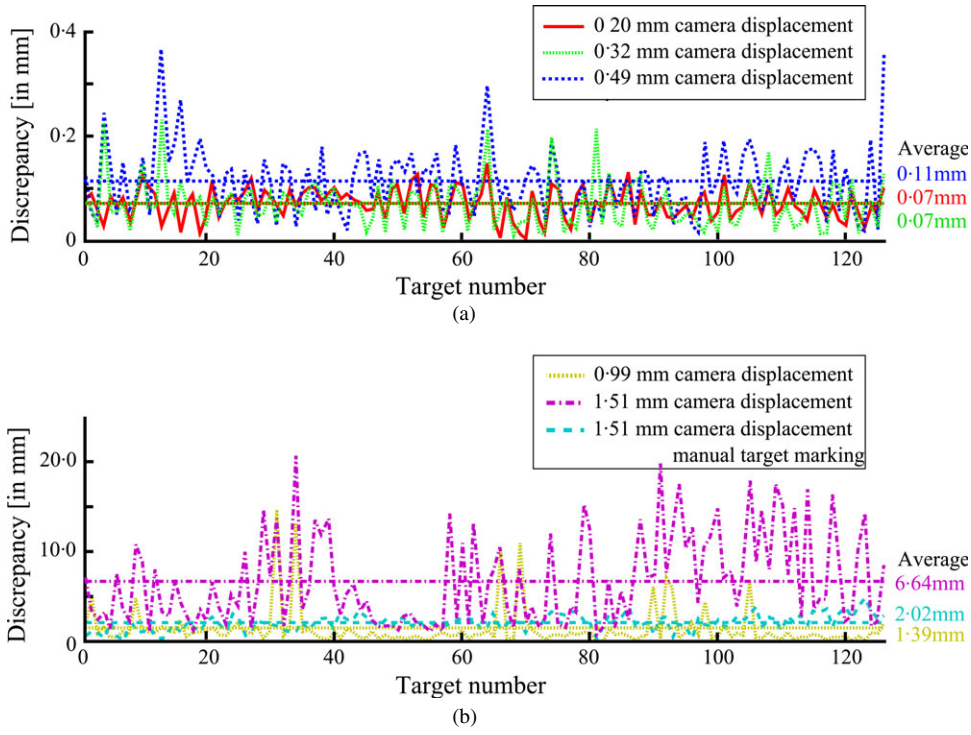

FIG. 12. Discrepancy between blurred and sharp image sets. The impact of large camera displacements (b) is 20 to 70 times larger than with small camera displacements (a).

detection to fail. The third dataset was used to determine a threshold beyond which blur disturbs the automatic detection of signalised targets (Fig. 13). The theoretical pixel size of a target is based on the focal length, the camera-to-object distance and the image sensor. In practice, the pixel width of a target can be counted on the image. In a sharp image, the theoretically calculated size and the actual size on the image should be equal. If the target is blurred, the pixel width in the image becomes larger than the theoretical size.

From the data captured it is possible to find the threshold at which detection fails due to blur. Determining the practical pixel width on the image and comparing it to the theoretical target width should make it possible to identify a linear dependency between sharp and blurred target sizes (Fig. 13(a)). The best-fitting linear dependency can be used to formulate an equation that describes the degree to which a target can be blurred before automatic detection is unsuccessful. A theoretical target size in pixels t_s can be determined easily using information about the target size in object space t_0, focal length c_k, distance between the camera and target h and sensor pixel size p_s. Furthermore, the blurred target size t_b can be related linearly to its theoretical equivalent t_s:

$$t_s = \frac{t_0 c_k}{h p_s}$$
$$t_b \leq 1{\cdot}166 t_s + 16{\cdot}794. \quad (1)$$

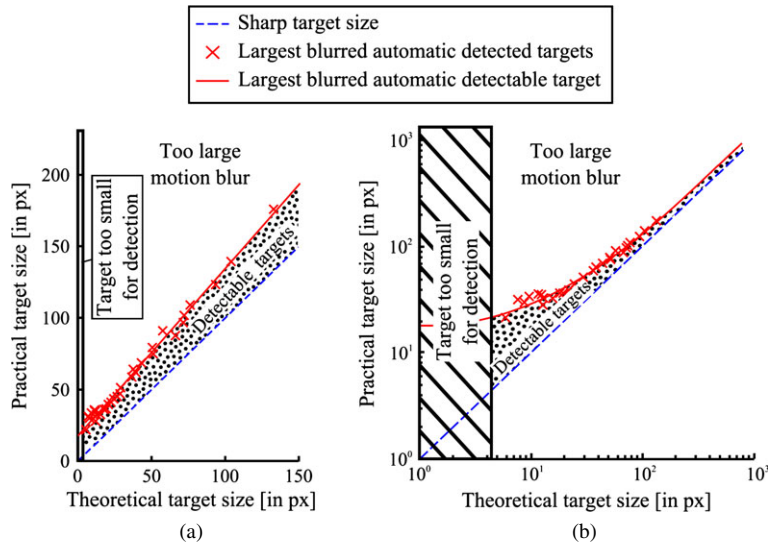

FIG. 13. Target size in a sharp image referenced to target size in a blurred image where automatic detection failed. Different camera models and lenses were used: (a) linear axes scale; (b) logarithmic axes scale.

From the tests conducted, targets which have a theoretical width of t_s, and appear in the image with a width between t_s and t_b, can be automatically detected. In Fig. 13(b) it is possible to see that the ratio between the theoretical and blurred target sizes decreases for larger targets. This implies that there is a greater tolerance to the blurring of small targets than that of large targets. A possible explanation is the threshold used in the detection algorithm. This threshold is based on the roundness of a target and how many pixels are part of a round target. For large targets an increased number of pixels do not support a round target and it is not accepted as a target.

The size of a blur is a direct result of camera displacement. Larger displacements cause targets to appear more smeared. Fig. 13 illustrates how much displacement is required for target detection to fail, and how wide the target appears in the image. Comparing camera displacement with the size of the blurred targets proves that large targets can be blurred more than small targets. Fig. 14 shows how target size, camera displacement and camera-to-object distance are related. The dependency between camera displacement and successful target detection is exponential, which shows that smaller targets tolerate more blur than larger targets. A target with a theoretical width of 50 pixels can be detected until it becomes so blurred that its width increases to 75 pixels, suggesting that a 50% blurring can be tolerated. However, a target measuring 100 pixels can be only smeared to 133 pixels before detection fails, which is only an increase of 33%. These examples suggest that the 50-pixel target can only suffer a displacement of 25 pixels before detection is unsuccessful, whilst the larger 100-pixel target can resist detection failure due to blur up to 33 pixels. This represents a difference of 8 pixels of additional camera displacement that can be tolerated if larger targets are used (Fig. 14). It also shows that an increasing object-to-camera distance results in a flatter exponential function. The outliers, which do not support the exponential function, are the smallest targets with a size of 4 mm. It would appear that the detection algorithm does not detect very small targets because they have too few pixels in the image

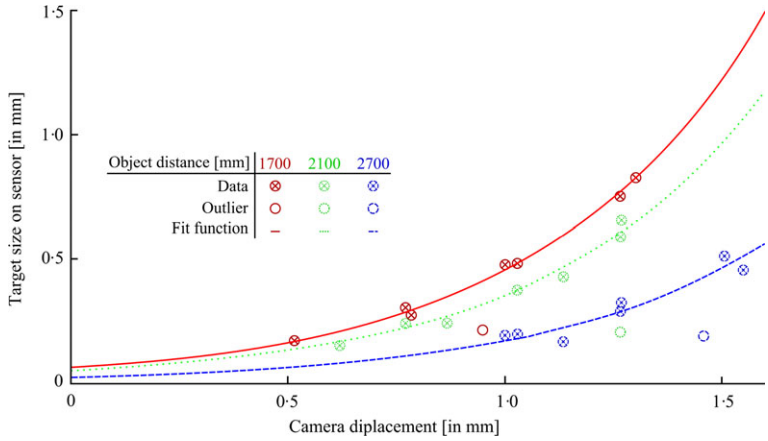

FIG. 14. Size of blurred targets related to displacement of the camera during shaking.

to be recognised as a target (Fig. 15(a)). However, once blurred they are represented by enough pixels to be accepted as a target (Fig. 15(b)). Notwithstanding this, as the target becomes more blurred, the detection fails again because the target shape becomes too elliptical and does not appear as a circle (Fig. 15(c)).

The function best representing the dependency between the camera-to-object distance, displacement and blurred target size, as shown in Fig. 14, is the exponential function shown in equation (2). This function makes it possible to calculate the blurred target size t_b as dependent on the camera-to-object distance h and the camera displacement d for short camera-to-object distances:

$$t_b = 70000h^{-1{\cdot}85}e^{2d}. \tag{2}$$

Equation (2) has not been investigated for $h \gg 3$ m and should be treated with caution for the increased camera-to-object distances that may be more common with UAVs. The displacement d is the result of the camera velocity during exposure time (equation (3)). Forward-motion displacement can be calculated using the exposure time and UAV velocity. In the case of rotations, the calculation depends on the position of the rotational axes. If the

(a) (b) (c)

FIG. 15. Influence of blur on small targets: (a) sharp target consists of too few pixels to be detected; (b) the same target when blurred, causing it to have an increased number of pixels; this target was detected by PhotoModeler; (c) the same target when even more blurred and no longer detectable by PhotoModeler.

origin of the axes is coincident with the camera's perspective centre, a calculation is possible using equation (3). As opposed to the roll ω and pitch φ, which only depend on the flight altitude, the yaw κ depends on the distance between the nadir position and the object s for which the displacement d is calculated:

$$\begin{aligned} d &= v_t \cdot ex \\ d &= h\tan(v_{\omega/\varphi}) \cdot ex \\ d_\kappa &= s\tan(v_\kappa) \cdot ex \end{aligned} \tag{3}$$

where d_κ is the displacement in yaw; $v_{t/\omega/\varphi/\kappa}$ are the respective velocities in translation, roll, pitch and yaw; and ex is the exposure time.

Connecting equations (1) and (2) makes it possible to calculate the minimum target size t_0 that should be used for the following parameters that are normally part of the flight planning: object distances h known a priori; focal length c_k; sensor pixel size p_s; and camera displacements d:

$$t_0 \geq \frac{70000h^{-1{\cdot}85}e^{2d}h - 16{\cdot}794hp_s}{1{\cdot}166c_k}. \tag{4}$$

However, the inverse calculation of determining displacement based on the size of a blurred target is not always valid. It would only be valid when the blurred target is on the threshold between successful and unsuccessful detection because this equation is based on the maximum size of blurred targets. If a less blurred target is used in this calculation the real camera displacement will be larger than the calculated displacement.

Discussion of Results and Implications for Photogrammetric Imagery

The study reported in this paper demonstrates that working with blurred images causes a range of challenges. First, it is difficult for the human eye to quantify the amount of blur in an image, especially if there is no image available for comparison. Second, automatic processing is clearly influenced by small motion blur and the number of detected signalised targets decreases. Even images of apparently high visual quality can cause problems if a small amount of blur is present. The number of measured targets directly influences the accuracy and ability of subsequent calculations including camera calibration and bundle adjustment. The detection of targets becomes more reliable with larger targets, which include more pixels to calculate accurately the target centre. Furthermore, the same amount of blur causes a single target to blur laterally, causing misdetection or multiple detection. However, very large targets are impractical for efficient photogrammetric data processing.

If automatic target detection is not possible, semi-automatic detection of targets over small areas can be successful. However, this is time consuming as these detection areas have to be defined manually and accurately. Even with well-defined detection areas, the detection fails with increasing blur. Manual measurement of targets is possible but the results are not as accurate as automatic measurements on sharp images.

A limitation of the detailed tests conducted in this study has been the focus on close-range images. Care needs to be exercised in assessing the implications of these findings for UAV imagery where flight altitudes are much larger than the distances used in these experiments and camera displacements are larger due to the flight velocity. Furthermore, the

ratios between the object distance and baseline are smaller than in the conducted experiments, which results in glancing ray intersections. The effect is that small changes in one coordinate measurement due to blur will have a correspondingly larger effect on the calculated 3D coordinates.

This study supports the findings made using subjective human opinions. Johnson and Casson (1995) proved that blur influences acuity. The current study also shows that blur influences photogrammetric image processing. Compared with human perception, image processing is more sensitive to blur. In addition, the detection of blurred simple structures, such as round targets, causes problems for automatic processes. Colombo et al. (1987) tested humans on the detection of structures in blurred images and found a decreasing ability to read text with increasing blur. However, the legibility of text is a much more complicated task than the detection of round targets.

This work supports the desirability of excluding blurred images from photogrammetric processing. Gülch (2012) recommends elimination of blurred images as a first step in UAV image processing. The findings also support the work of Shah and Schickler (2012) who develop blur correction methods specifically for UAV applications. Lelégard et al. (2012) state that a blur larger than 2 pixels is a significant amount. However, the findings reported in this paper suggest that a blur of just 2 pixels is actually too small to influence the detection, identification, referencing and measurement of targets.

Conclusions

A range of difficulties concerning photogrammetric applications is caused by image degradation due to motion blur. Small camera displacements have a significant impact on the accuracy of subsequent calculations and processes. Activating a shutter button on a camera can result in significant camera movement causing image blur. Fully automatic detection of targets in images containing small blurs can be difficult and can influence further processing. This problem can be solved by using semi-automatic detection tools. A small amount of blur has no significant influence on calculation results when targets are detected and measured successfully. If blur increases to such a degree that semi-automatic detection requires significant operator input, subsequent calculation will return significantly inaccurate results. However, manual measurements can be carried out and results of acceptable accuracy can be achieved, even in highly blurred images. It is also important to recognise that the tests were conducted only using signalised targets. It can be assumed that using natural feature points results in fewer detected features and feature referencing can be erroneous or even becomes impossible. Using natural features for processing blurred images would be an interesting topic for future work.

Although blur might disturb most image processing procedures it can be also exploited for some applications, as identified by Boracchi (2009) and McCarthy et al. (2013).

References

Boracchi, G., 2009. Estimating the 3D direction of a translating camera from a single motion-blurred image. *Pattern Recognition Letters*, 30(7): 671–681.

Boracchi, G., Caglioti, V. and Giusti, A., 2007. Ball position and motion reconstruction from blur in a single perspective image. *14th International Conference on Image Analysis and Processing ICIAP 2007*, Modena, Italy. Pages 87–92.

Colombo, E. M., Kirschbaum, C. F. and Raitelli, M., 1987. Legibility of texts: the influence of blur. *Lighting Research and Technology*, 19(3): 61–71.

Eisenbeiss, H., 2009. *UAV photogrammetry*. Doctoral thesis 18515 ETH, Zurich, Switzerland. 235 pages.

EISENBEISS, H., 2011. *Tutorial on UAV-g: introduction*. Presentation at UAV-g 2011, Zurich, Switzerland. http://www.geometh.ethz.ch/uav_g/tutorial/eisenbeiss_web [Accessed: 7th October 2014].

EISENBEISS, H. and SAUERBIER, M., 2011. Investigation of UAV systems and flight modes for photogrammetric applications. *Photogrammetric Record*, 26(136): 400–421.

GRENZDÖRFFER, G., NIEMEYER, F. and SCHMIDT, F., 2012. Development of four vision camera system for a micro-UAV. *International Archives of Photogrammetry, Remote Sensing and Spatial Information Sciences*, 39(B1): 369–374.

GÜLCH, E., 2012. Photogrammetric measurements in fixed wing UAV imagery. *International Archives of Photogrammetry, Remote Sensing and Spatial Information Sciences*, 39(B1): 381–386.

JOHNSON, C. A. and CASSON, E. J., 1995. Effects of luminance, contrast, and blur on visual acuity. *Optometry and Vision Science*, 72(12): 864–869.

JOSHI, N., SZELISKI, R. and KRIEGMAN, D. J., 2008. PSF estimation using sharp edge prediction. *IEEE Conference on Computer Vision and Pattern Recognition*, Anchorage, Alaska, USA. 8 pages. http://dx.doi.org/10.1109/CVPR.2008.4587834

KIM, S. K. and PAIK, J. K., 1998. Out-of-focus blur estimation and restoration for digital auto-focusing system. *Electronics Letters*, 34(12): 1217–1219.

KRAUS, K., 2004. *Photogrammetrie*. Seventh edition. De Gruyter, Berlin, Germany. 516 pages.

KRAUS, K., 2007. *Photogrammetry – Geometry from Images and Laser Scans*. Second edition. De Gruyter, Berlin, Germany. 459 pages.

LELÉGARD, L., DELAYGUE, E., BRÉDIF, M. and VALLET, B., 2012. Detecting and correcting motion blur from images shot with channel-dependent exposure time. *ISPRS Annals of Photogrammetry, Remote Sensing and Spatial Information Sciences*, 1(3): 341–346.

LIU, R., LI, Z. and JIA, J., 2008. Image partial blur detection and classification. *IEEE Conference on Computer Vision and Pattern Recognition*, Anchorage, Alaska, USA. 8 pages. http://dx.doi.org/10.1109/CVPR.2008.4587465

LUHMANN, T., 2014. Eccentricity in images of circular and spherical targets and its impact on spatial intersection. *Photogrammetric Record*, 29(148): 417–433.

LUHMANN, T., ROBSON, S., KYLE, S. and BOEHM, J., 2014. *Close-Range Photogrammetry and 3D Imaging*. Second edition. De Gruyter, Berlin, Germany. 684 pages.

MAISON NICÉPHORE NIÉPCE, 2013. http://www.niepce.org/pagus/pagus-inv.html [Accessed: 24th June 2013].

MCCARTHY, D. M. J., CHANDLER, J. H. and PALMERI, A., 2013. Monitoring dynamic structural tests using image deblurring techniques. *Key Engineering Materials, Damage Assessment of Structures X*, 569–570: 932–939.

NARVEKAR, N. D. and KARAM, L. J., 2009. *A no-reference perceptual image sharpness metric based on a cumulative probability of blur detection*. International Workshop on Quality of Multimedia Experience, San Diego, California, USA. Pages 87–91.

ONG, E., LIN, W., LU, Z., YANG, X., YAO, S., PAN, F., JIANG, L. and MOSCHETTI, F., 2003. A no-reference quality metric for measuring image blur. *Seventh International Symposium on Signal Processing and its Applications*, Paris, France. 1: 469–472.

PACEY, R. and FRICKER, P., 2005. Forward motion compensation (FMC) – is it the same in the digital imaging world? *Photogrammetric Engineering & Remote Sensing*, 71(11): 1241–1242.

RAHTU, E., HEIKKILÄ, J., OJANSIVU, V. and AHONEN, T., 2012. Local phase quantization for blur-insensitive image analysis. *Image and Vision Computing*, 30(8): 501–512.

SACHS, D., NASIRI, S. and GOEHL, D., 2006. *Image stabilization technology overview*. http://www.invensense.com/jp/mems/gyro/documents/whitepapers/ImageStabilizationWhitepaper_051606.pdf [Accessed: 29th October 2013].

SHAH, C. A. and SCHICKLER, W., 2012. Automated blur detection and removal in airborne imaging systems using IMU data. *International Archives of Photogrammetry, Remote Sensing and Spatial Information Sciences*, 39(B1): 321–323.

SHAKED, D. and TASTL, I., 2005. Sharpness measure: towards automatic image enhancement. *IEEE International Conference on Image Processing*, Genoa, Italy. I: 937–940.

SHORTIS, M. R. and SEAGER, J. W., 2014. A practical target recognition system for close range photogrammetry. *Photogrammetric Record*, 29(147): 337–355.

SIEBERTH, T., WACKROW, R. and CHANDLER, J. H., 2013. Automatic isolation of blurred images from UAV image sequences. *International Archives of Photogrammetry, Remote Sensing and Spatial Information Sciences*, 40(1/W2): 361–366.

STILES, R. N., 1976. Frequency and displacement amplitude relations for normal hand tremor. *Journal of Applied Physiology*, 40(1): 44–54.

Résumé

Les drones sont devenus un sujet de recherche intéressant et dynamique en photogrammétrie. Les recherches actuelles s'intéressent à des images acquises depuis des drones qui permettent une haute résolution spatiale et spectrale grâce à un vol à basse altitude et à des caméras à haute résolution. L'un des principaux problèmes empêchant l'automatisation du traitement des images acquises par drone est la méconnaissance de l'effet du phénomène de filé produit par le mouvement de la caméra durant l'acquisition des images. L'objet de cet article est d'analyser l'influence du filé sur le traitement photogrammétrique des images. Des images ont été produites avec un effet de filé parfaitement connu pour en déterminer l'influence. On constate que même des filés très limités affectent de manière significative le traitement photogrammétrique. Une intervention de l'opérateur, bien que coûteuse en temps, permet de garantir des résultats de qualité acceptable.

Zusammenfassung

Unbemannte Luftfahrzeuge (UAV) sind ein interessantes und aktuelles Thema in der photogrammetrischen Forschung. Die mit den UAVs aufgenommenen Bilder weisen, aufgrund der geringen Flughöhe und der Nutzung hochauflösender Kameras, eine hohe geometrische und spektrale Auflösung auf. Es wird angenommen, dass die Bewegungsunschärfe die vollautomatische photogrammetrische Auswertung von UAV Bildern beeinträchtigt. Bisher ist jedoch unbekannt, in welchem Maße unscharfe Bilder den Prozess beeinflussen. Ziel dieser Veröffentlichung ist es, den Einfluss von Bewegungsunschärfe auf photogrammetrische Prozesse zu untersuchen. Dazu werden Bilder mit genau bekannter Bewegungsunschärfe erzeugt, um deren Einfluss auf photogrammetrische Operationen zu analysieren. Es wurde herausgefunden, dass schon eine geringe Unschärfe den Verlauf photogrammetrischer Prozeduren negativ beeinflusst. Manuelle Eingriffe können zwar akzeptable Ergebnisse sicherstellen, sind jedoch sehr zeitintensiv.

Resumen

Los vehículos aéreos no tripulados (UAV) se han convertido en un interesante y activo tema de investigación en fotogrametría. La presente investigación está basada en imágenes captadas desde UAVs que tienen una alta resolución espacial y buena resolución espectral gracias a la combinación de vuelos a baja altitud con cámaras de alta resolución. Uno de los principales problemas que dificultan la automatización del proceso de datos de imágenes de UAV es el efecto de la degradación en la definición ocasionado por el movimiento de la cámara durante la adquisición. El propósito de este trabajo es analizar la influencia de esta falta de definición en el proceso de imágenes fotogramétricas. Se producen imágenes con degradación de la definición causado por el movimiento conocida para determinar su efecto. Se encontró que incluso pequeñas degradaciones de la definición afectan significativamente a los procesos normales fotogramétricos. Aunque la intervención manual conlleva mucho tiempo sin embargo puede garantizar resultados aceptables.

摘要

无人机已经成为摄影测量领域一个非常活跃的研究方向,现在的研究主要集中在利用低空飞行无人机配备的高分相机获取高空间分辨率和高光谱分辨率遥感影。现在阻碍无人机影像全自动化处理的主要问题是在影像采集过程由于相机运动引起的模糊。本文分析了该类模糊对摄影测量影像处理的影响,结果表明,小的模糊对摄影测量处理的影响是非常大的。虽然操作员人机交互可能比较耗费时间,但是齐可以确保处理结果达到可接受的摄影测量精度。